Available online at www.sciencedirect.com

SCIENCE DIRECT®

Electric Power Systems Research 75 (2005) 142–152

ELECTRIC POWER SYSTEMS RESEARCH

www.elsevier.com/locate/epsr

Rotor flux oriented control of a symmetrical six-phase induction machine

S.N. Vukosavic, M. Jones, E. Levi, J. Varga*

Abstract

Basic concepts of six-phase ac motor drives have been in existence for a number of years and were considered extensively in the eighties for safety-critical and/or high power applications. There has been an upsurge in the interest in these drives in recent times, initiated by various application areas, such as 'more-electric' aircraft, electric ship propulsion and EV/HVs. All the existing work considers an asymmetrical six-phase ac machine, with two sets of three-phase windings shifted in space by 30° (dual three-phase, split-phase, double star). In contrast to this general trend, a symmetrical six-phase induction machine, with spatial displacement between any two consecutive phases equal to 60°, is discussed in this paper. A vector control algorithm, based on indirect rotor flux orientation, is at first briefly described. Special attention is paid next to the current control issue, from the point of view of the minimum number of current controllers. An overview of the experimental test bench that utilises phase current control in the stationary reference frame is further given. Attainable performance is analysed experimentally and the results are presented for a number of operating regimes, including acceleration, deceleration, reversing and step loading/unloading transients. It is demonstrated that the achievable quality of high performance is excellent, while the standard benefits of the multiphase motor drives are retained.

Keywords: Current control; Rotor flux oriented control; Six-phase induction machine

1. Introduction

One of the first proposals of a multiphase variable speed electric drive dates back to 1969 [1]. While [1] dealt with a five-phase induction machine, six-phase (double star) induction machine supplied from a six-phase inverter was examined in [2,3]. The early interest in multiphase machines was caused by the possibility of reducing the torque ripple in inverter fed drives (operated in 180° conduction mode), when compared to the three-phase case. Another advantage of a multiphase motor drive over a three-phase motor drive is the improved reliability [4–7]. Fault tolerance is one of the main reasons behind the application of six-phase (double star) and nine-phase (triple star) induction motor drives in locomotives [4,5]. The other main reason is that for a given motor power an increase of the number of phases enables reduction of the power per phase, which translates into a reduction of the power per inverter leg. Multiphase machines are therefore often considered for and applied in high power applications.

Recent developments in the areas of 'more-electric' aircraft, electric ship propulsion and EV/HVs have led to a substantial increase in the research effort put into development of multiphase high performance drive systems. One of the most frequently considered drive structures is based on utilisation of a six-phase ac machine [8–17]. The machine type depends on the target application. By far the most frequent are the induction motor drives [9,10,12–17], primarily

* Corresponding author. Tel.: +44 151 231 2257; fax: +44 151 298 2624.
E-mail addresses: e.levi@livjm.ac.uk (E. Levi)

discussed in the context of high power applications. Permanent magnet synchronous motor drives [8,11] are usually considered for safety critical applications.

Detailed studies of induction machine configurations with multiple sets of three-phase stator windings and with an arbitrary number of phases have been conducted in [18] and [19], respectively. It was concluded in [18] that, in the case of a six-phase induction machine, it is advantageous to use an asymmetrical stator winding structure, with two three-phase windings spatially shifted by 30°, instead of a symmetrical winding structure with a 60° spatial shift between any two consecutive phases. The background thinking behind this conclusion is related to the pre-PWM era of VSI control, when 180° conduction mode was utilised. By using an asymmetrical six-phase machine it became possible to eliminate the sixth harmonic from the torque ripple. An asymmetrical six-phase induction motor drive has been utilised ever since, as evidenced by the surveyed references.

The main problem encountered in actual implementation of vector controlled asymmetrical six-phase induction motors is the existence of harmonic currents of the order $6n \pm 1$ ($n = 1, 3, 5, \ldots$), which do not contribute to the torque and air-gap flux production but can freely flow in the machine [14–17]. In addition to these non-torque producing currents, an asymmetrical six-phase machine with a single star point allows the flow of the triple harmonics of the order $3n$ as well. This is the reason why star points of the two three-phase windings are normally kept isolated. On the other hand, utilisation of a single star point enables enhancement of the torque production by means of the third-harmonic stator current injection [11,12]. This, however, requires connection of the star point to the mid-point of the dc-bus split-capacitor arrangement and can cause some problems due to the third harmonic current flow through the capacitors [12].

Proper control is further jeopardised by unbalanced current sharing between the two three-phase winding sets, caused by inherent asymmetries in the machine [12,13]. It is for these reasons that the standard current control in the rotating reference frame, where only stator d–q currents are regulated, does not yield a satisfactory performance of the drive. The problem can be solved by modifying the current control scheme in the rotating reference frame [20], by using four stationary current controllers in α–β and x–y sub-spaces, as discussed in [13], or by employing an advanced space vector modulation (SVM) scheme in conjunction with d–q current controllers, which ensures non-existence of voltage harmonics in the x–y sub-space [14].

In contrast to the existing solutions, this paper considers vector control of a symmetrical six-phase induction machine, with a single, isolated star point. The advantage of a single star point, when compared to the isolated double star arrangement, is an improved fault tolerance (since there are five independent currents rather than two pairs of independent currents). In order to avoid the problems associated with potential flow of harmonics of the orders $6n \pm 1$ ($n = 1, 3, 5, \ldots$) and $3n$, current control in the stationary reference frame, using machine's phase currents, is implemented.

It is demonstrated by means of experimental results that the quality of dynamic performance attainable with the proposed control scheme is excellent. Spectral analysis of the stator current shows that the unwanted low order harmonics practically do not exist or are of negligibly small values. The drive simultaneously retains the good features of multiphase motor drives, such as a reduced rating per inverter leg for given motor power and fault tolerance.

2. Configuration of the drive

Schematic illustration of the symmetrical six-phase induction motor drive is shown in Fig. 1. As already noted, spatial displacement between any two consecutive stator phases is 60° and there is a single star point. The drive is supplied from a six-phase current controlled voltage source inverter (VSI). Inverter phase current references are generated by the indirect vector controller, as explained later. Current control is exercised in the stationary reference frame, using phase currents. The reasoning behind this choice of the current control scheme will be explained in the next section, upon machine model development.

3. Modelling of the six-phase induction motor

3.1. Phase-variable model

The electrical sub-system's model of the drive in Fig. 1 is of the 12th order, since rotor cage winding is considered as a symmetrical six-phase winding as well. It can be given in matrix form with

$$\underline{v} = \underline{R}\,\underline{i} + \frac{\mathrm{d}(\underline{L}\,\underline{i})}{\mathrm{d}t}, \tag{1}$$

where

$$\underline{v} = \begin{bmatrix} \underline{v}^{\mathrm{INV}} & \underline{0} \end{bmatrix}^{\mathrm{T}} \qquad \underline{i} = \begin{bmatrix} \underline{i}^{\mathrm{INV}} & \underline{i}_{\mathrm{r}} \end{bmatrix}^{\mathrm{T}}. \tag{2}$$

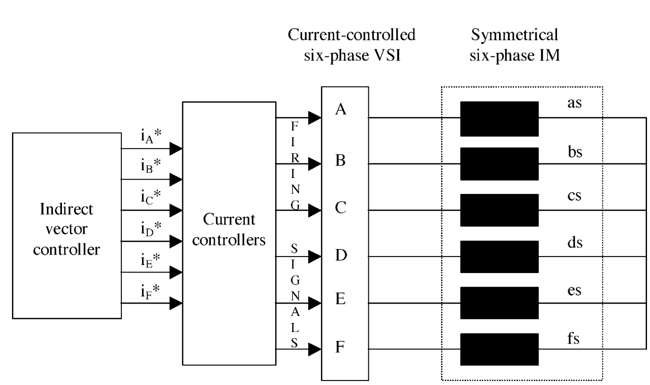

Fig. 1. Symmetrical six-phase vector controlled induction motor drive.

and voltage and current vectors are

$$\underline{v}^{\mathrm{INV}} = \begin{bmatrix} v_{\mathrm{A}} \\ v_{\mathrm{B}} \\ v_{\mathrm{C}} \\ v_{\mathrm{D}} \\ v_{\mathrm{E}} \\ v_{\mathrm{F}} \end{bmatrix} = \begin{bmatrix} v_{\mathrm{as}} \\ v_{\mathrm{bs}} \\ v_{\mathrm{cs}} \\ v_{\mathrm{ds}} \\ v_{\mathrm{es}} \\ v_{\mathrm{fs}} \end{bmatrix} \qquad \underline{i}_{\mathrm{s}} = \begin{bmatrix} i_{\mathrm{as}} \\ i_{\mathrm{bs}} \\ i_{\mathrm{cs}} \\ i_{\mathrm{ds}} \\ i_{\mathrm{es}} \\ i_{\mathrm{fs}} \end{bmatrix} = \begin{bmatrix} i_{\mathrm{A}} \\ i_{\mathrm{B}} \\ i_{\mathrm{C}} \\ i_{\mathrm{D}} \\ i_{\mathrm{E}} \\ i_{\mathrm{F}} \end{bmatrix} = \underline{i}^{\mathrm{INV}} \tag{3}$$

$$\underline{i}_{\mathrm{r}} = \begin{bmatrix} i_{\mathrm{ar}} & i_{\mathrm{br}} & i_{\mathrm{cr}} & i_{\mathrm{dr}} & i_{\mathrm{er}} & i_{\mathrm{fr}} \end{bmatrix}^{\mathrm{T}}. \tag{4}$$

Matrix voltage Equation (1) can be given as

$$\begin{bmatrix} \underline{v}^{\mathrm{INV}} \\ \underline{0} \end{bmatrix} = \begin{bmatrix} \underline{R}_{\mathrm{s}} & \\ & \underline{R}_{\mathrm{r}} \end{bmatrix} \begin{bmatrix} \underline{i}^{\mathrm{INV}} \\ \underline{i}_{r} \end{bmatrix} + \frac{\mathrm{d}}{\mathrm{d}t}\left\{ \begin{bmatrix} \underline{L}_{\mathrm{s}} & \underline{L}_{\mathrm{sr}} \\ \underline{L}_{\mathrm{rs}} & \underline{L}_{\mathrm{r}} \end{bmatrix} \begin{bmatrix} \underline{i}^{\mathrm{INV}} \\ \underline{i}_{\mathrm{r}} \end{bmatrix} \right\}. \tag{5}$$

All the parameter sub-matrices are of 6×6 dimensions. Machine's electromagnetic torque can be expressed as

$$\begin{aligned} T_{\mathrm{e}} = -PM\{&(i_{\mathrm{A}}i_{\mathrm{ar}} + i_{\mathrm{B}}i_{\mathrm{br}} + i_{\mathrm{C}}i_{\mathrm{cr}} + i_{\mathrm{D}}i_{\mathrm{dr}} + i_{\mathrm{E}}i_{\mathrm{er}} + i_{\mathrm{F}}i_{\mathrm{fr}}) \\ &\times \sin\theta + (i_{\mathrm{F}}i_{\mathrm{ar}} + i_{\mathrm{A}}i_{\mathrm{br}} + i_{\mathrm{B}}i_{\mathrm{cr}} + i_{\mathrm{C}}i_{\mathrm{dr}} + i_{\mathrm{D}}i_{\mathrm{er}} + i_{\mathrm{E}}i_{\mathrm{fr}}) \\ &\times \sin(\theta - 5\alpha) + (i_{\mathrm{E}}i_{\mathrm{ar}} + i_{\mathrm{F}}i_{\mathrm{br}} + i_{\mathrm{A}}i_{\mathrm{cr}} + i_{\mathrm{B}}i_{\mathrm{dr}} + i_{\mathrm{C}}i_{\mathrm{er}} \\ &+ i_{\mathrm{D}}i_{\mathrm{fr}})\sin(\theta - 4\alpha) + (i_{\mathrm{D}}i_{\mathrm{ar}} + i_{\mathrm{E}}i_{\mathrm{br}} + i_{\mathrm{F}}i_{\mathrm{cr}} + i_{\mathrm{A}}i_{\mathrm{dr}} \\ &+ i_{\mathrm{B}}i_{\mathrm{er}} + i_{\mathrm{C}}i_{\mathrm{fr}})\sin(\theta - 3\alpha) + (i_{\mathrm{C}}i_{\mathrm{ar}} + i_{\mathrm{D}}i_{\mathrm{br}} + i_{\mathrm{E}}i_{\mathrm{cr}} \\ &+ i_{\mathrm{F}}i_{\mathrm{dr}} + i_{\mathrm{A}}i_{\mathrm{er}} + i_{\mathrm{B}}i_{\mathrm{fr}})\sin(\theta - 2\alpha) + (i_{\mathrm{B}}i_{\mathrm{ar}} + i_{\mathrm{C}}i_{\mathrm{br}} \\ &+ i_{\mathrm{D}}i_{\mathrm{cr}} + i_{\mathrm{E}}i_{\mathrm{dr}} + i_{\mathrm{F}}i_{\mathrm{er}} + i_{\mathrm{A}}i_{\mathrm{fr}})\sin(\theta - \alpha)\}. \end{aligned} \tag{6}$$

Angle θ denotes instantaneous rotor position. Equations (5) and (6) are further transformed using decoupling transformation matrix.

3.2. Application of the decoupling transformation

The correlation between original phase variables and new variables is given with $\underline{f}_{\alpha\beta} = \underline{C}\,\underline{f}_{\mathrm{abcdef}}$, where $\underline{C}$ is the power-invariant transformation matrix

$$\underline{C} = \sqrt{\frac{2}{6}} \begin{array}{c} \alpha \\ \beta \\ x \\ y \\ 0+ \\ 0- \end{array} \left|\, \begin{bmatrix} 1 & \cos\alpha & \cos 2\alpha & \cos 3\alpha & \cos 4\alpha & \cos 5\alpha \\ 0 & \sin\alpha & \sin 2\alpha & \sin 3\alpha & \sin 4\alpha & \sin 5\alpha \\ 1 & \cos 2\alpha & \cos 4\alpha & \cos 6\alpha & \cos 8\alpha & \cos 10\alpha \\ 0 & \sin 2\alpha & \sin 4\alpha & \sin 6\alpha & \sin 8\alpha & \sin 10\alpha \\ 1/\sqrt{2} & 1/\sqrt{2} & 1/\sqrt{2} & 1/\sqrt{2} & 1/\sqrt{2} & 1/\sqrt{2} \\ 1/\sqrt{2} & -1/\sqrt{2} & 1/\sqrt{2} & -1/\sqrt{2} & 1/\sqrt{2} & -1/\sqrt{2} \end{bmatrix}\right., \tag{7}$$

and $\alpha = 60°$. Application of the transformation matrix (7) in conjunction with (5) and (6) leads to the decoupled model of the symmetrical six-phase induction motor drive. Inverter (stator) voltage equations can be expressed as

$$\begin{aligned} v_{\alpha}^{\mathrm{INV}} &= R_{\mathrm{s}}i_{\alpha}^{\mathrm{INV}} + L_{\mathrm{s}}\frac{\mathrm{d}i_{\alpha}^{\mathrm{INV}}}{\mathrm{d}t} + L_{\mathrm{m}}\frac{\mathrm{d}}{\mathrm{d}t}(\cos\theta i_{\alpha\mathrm{r}} - \sin\theta i_{\beta\mathrm{r}}) \\ v_{\beta}^{\mathrm{INV}} &= R_{\mathrm{s}}i_{\beta}^{\mathrm{INV}} + L_{\mathrm{s}}\frac{\mathrm{d}i_{\beta}^{\mathrm{INV}}}{\mathrm{d}t} + L_{\mathrm{m}}\frac{\mathrm{d}}{\mathrm{d}t}(\sin\theta i_{\alpha\mathrm{r}} + \cos\theta i_{\beta\mathrm{r}}) \\ v_{x}^{\mathrm{INV}} &= R_{\mathrm{s}}i_{x}^{\mathrm{INV}} + L_{ls}\frac{\mathrm{d}i_{x}^{\mathrm{INV}}}{\mathrm{d}t} \\ v_{y}^{\mathrm{INV}} &= R_{\mathrm{s}}i_{y}^{\mathrm{INV}} + L_{ls}\frac{\mathrm{d}i_{y}^{\mathrm{INV}}}{\mathrm{d}t} \\ v_{0+}^{\mathrm{INV}} &= R_{\mathrm{s}}i_{0+}^{\mathrm{INV}} + L_{ls}\frac{\mathrm{d}i_{0+}^{\mathrm{INV}}}{\mathrm{d}t} \\ v_{0-}^{\mathrm{INV}} &= R_{\mathrm{s}}i_{0-}^{\mathrm{INV}} + L_{ls}\frac{\mathrm{d}i_{0-}^{\mathrm{INV}}}{\mathrm{d}t} \end{aligned} \tag{8}$$

where magnetising inductance is $L_{\mathrm{m}} = 3M$, index l stands for leakage inductances and L_{s}, L_{r} are stator and rotor winding self-inductance.

Rotor voltage equations take the form:

$$\begin{aligned} 0 &= R_{\mathrm{r}}i_{\alpha\mathrm{r}} + L_{\mathrm{r}}\frac{\mathrm{d}i_{\alpha r}}{\mathrm{d}t} + \frac{\mathrm{d}}{\mathrm{d}t}L_{\mathrm{m}}(\cos\theta i_{\alpha}^{\mathrm{INV}} + \sin\theta i_{\beta}^{\mathrm{INV}}) \\ 0 &= R_{\mathrm{r}}i_{\beta\mathrm{r}} + L_{\mathrm{r}}\frac{\mathrm{d}i_{\beta\mathrm{r}}}{\mathrm{d}t} + \frac{\mathrm{d}}{\mathrm{d}t}L_{\mathrm{m}}(-\sin\theta i_{\alpha}^{\mathrm{INV}} + \cos\theta i_{\beta}^{\mathrm{INV}}). \\ 0 &= R_{\mathrm{r}}i_{k} + L_{l\mathrm{r}}\frac{\mathrm{d}i_{k}}{\mathrm{d}t} \quad k = xr,\ yr,\ 0+,\ 0- \end{aligned} \tag{9}$$

Application of the decoupling transformation on the torque Equation (6) yields

$$\begin{aligned} T_{\mathrm{e}} = PL_{\mathrm{m}}[&\cos\theta(i_{\alpha\mathrm{r}}i_{\beta}^{\mathrm{INV}} - i_{\beta\mathrm{r}}i_{\alpha}^{\mathrm{INV}}) \\ &- \sin\theta(i_{\alpha\mathrm{r}}i_{\alpha}^{\mathrm{INV}} + i_{\beta\mathrm{r}}i_{\beta}^{\mathrm{INV}})] \end{aligned} \tag{10}$$

According to (8)–(10), flux/torque producing stator currents of the symmetrical six-phase machine are the inverter α–β current components, while the x–y and 0+, 0− are non-air-gap flux/torque producing stator currents. Since rotor is short circuited, x–y and 0+, 0− circuits cannot be exited and these equations in (9) can be omitted from further considerations.

Stator voltage Equation (8) shows that, in general, it is not sufficient to control only two flux/torque producing stator current components. If the inverter produces such voltages that x–y stator voltage components exist (i.e., there are voltage harmonics of the order $6n \pm 1$ ($n = 1, 3, 5, \ldots$)), stator current x–y components will freely flow. Further, since there is only one star point, the 0− component of the stator current can freely flow as well if the inverter produces harmonics of the order $3n$. There are therefore five independent currents (this can be reduced to four, by disconnecting the star points of the two three-phase windings, since 0− component of the stator current then cannot flow). Due to the similarity between symmetrical and asymmetrical six-phase machine, the same conclusions apply to the asymmetrical six-phase machine. As already noted, the problem can be alleviated for asymmetrical six-phase machines with isolated star points by using two pairs of stationary current controllers (α–β and x–y) as in [13], by modifying the synchronous reference frame current control through introduction of appropriate compensating terms [20], or by devising a proper SVM scheme, which ensures that voltage harmonics in the x–y sub-space are nullified.

3.3. Model in the stationary common reference frame

Rotational transformation, leading to the d–q system of equations, is applied next in conjunction with rotor equations. The matrix has for the six-phase machine the following form:

$$\underset{\sim}{D}_{\mathrm{r}} = \begin{bmatrix} \cos\theta & -\sin\theta & \\ \sin\theta & \cos\theta & \\ & & [\underset{\sim}{I}]^{4\times 4} \end{bmatrix}, \tag{11}$$

where $\underset{\sim}{I}$ is the diagonal 4×4 unity matrix. As already noted, equations determined with this part of the transformation can be omitted from further considerations. Upon application of the rotational transformation the voltage equations for stator and rotor, respectively, become

$$\begin{aligned} v_d^{\mathrm{INV}} &= R_{\mathrm{s}} i_d^{\mathrm{INV}} + L_{\mathrm{s}} \frac{\mathrm{d}i_d^{\mathrm{INV}}}{\mathrm{d}t} + L_{\mathrm{m}} \frac{\mathrm{d}i_{d\mathrm{r}}}{\mathrm{d}t} \\ v_q^{\mathrm{INV}} &= R_{\mathrm{s}} i_q^{\mathrm{INV}} + L_{\mathrm{s}} \frac{\mathrm{d}i_q^{\mathrm{INV}}}{\mathrm{d}t} + L_{\mathrm{m}} \frac{\mathrm{d}i_{q\mathrm{r}}}{\mathrm{d}t} \\ v_x^{\mathrm{INV}} &= R_{\mathrm{s}} i_x^{\mathrm{INV}} + L_{l\mathrm{s}} \frac{\mathrm{d}i_x^{\mathrm{INV}}}{\mathrm{d}t} \\ v_y^{\mathrm{INV}} &= R_{\mathrm{s}} i_y^{\mathrm{INV}} + L_{l\mathrm{s}} \frac{\mathrm{d}i_y^{\mathrm{INV}}}{\mathrm{d}t} \\ v_{0+}^{\mathrm{INV}} &= R_{\mathrm{s}} i_{0+}^{\mathrm{INV}} + L_{l\mathrm{s}} \frac{\mathrm{d}i_{0+}^{\mathrm{INV}}}{\mathrm{d}t} \\ v_{0-}^{\mathrm{INV}} &= R_{\mathrm{s}} i_{0-}^{\mathrm{INV}} + L_{l\mathrm{s}} \frac{\mathrm{d}i_{0-}^{\mathrm{INV}}}{\mathrm{d}t} \end{aligned}, \tag{12}$$

$$\begin{aligned} 0 &= R_{\mathrm{r}} i_{d\mathrm{r}} + L_{\mathrm{m}} \frac{\mathrm{d}i_d^{\mathrm{INV}}}{\mathrm{d}t} + L_{\mathrm{r}} \frac{\mathrm{d}i_{d\mathrm{r}}}{\mathrm{d}t} + \omega(L_{\mathrm{m}} i_q^{\mathrm{INV}} + L_{\mathrm{r}} i_{q\mathrm{r}}) \\ 0 &= R_{\mathrm{r}} i_{q\mathrm{r}} + L_{\mathrm{m}} \frac{\mathrm{d}i_q^{\mathrm{INV}}}{\mathrm{d}t} + L_{\mathrm{r}} \frac{\mathrm{d}i_{q\mathrm{r}}}{\mathrm{d}t} - \omega(L_{\mathrm{m}} i_d^{\mathrm{INV}} + L_r i_{d\mathrm{r}}) \end{aligned}, \tag{13}$$

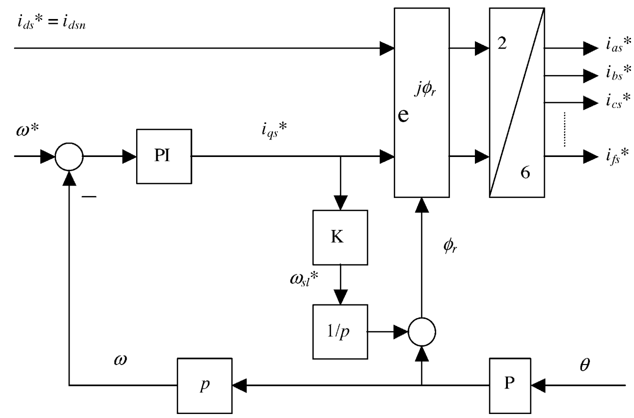

Fig. 2. Indirect (feed-forward) rotor flux oriented controller for a symmetrical six-phase induction machine ($K_1 = 1/(T_{\mathrm{r}}^* i_{\mathrm{ds}}^*)$, $p \equiv \mathrm{d}/\mathrm{d}t$).

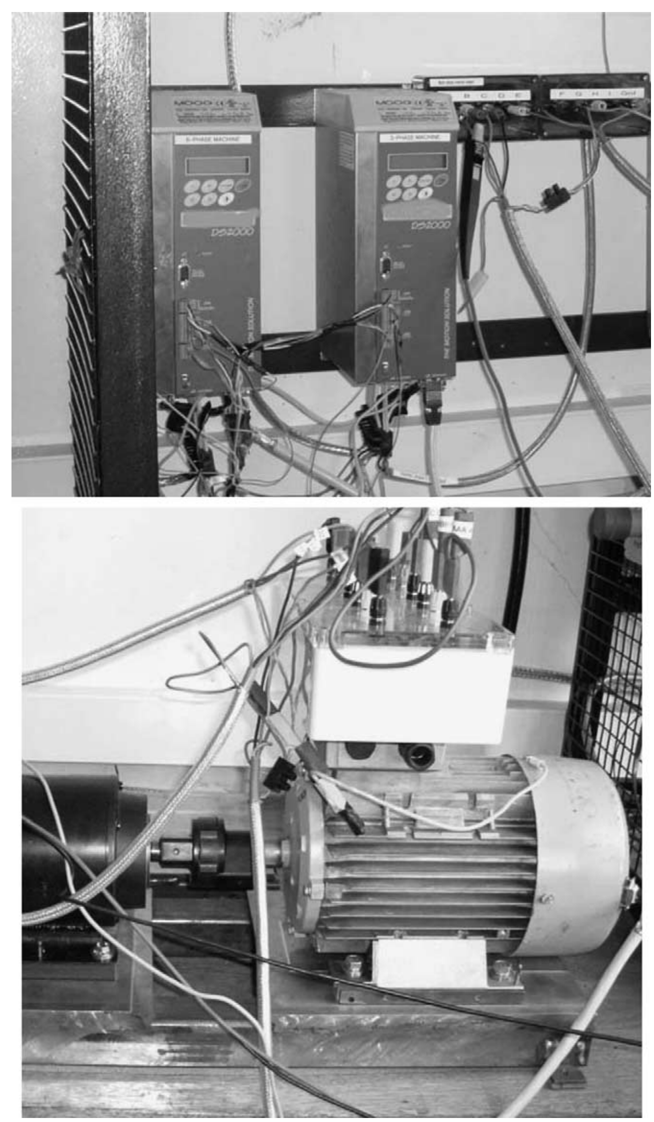

Fig. 3. Experimental test bench: the two three-phase inverters and the symmetrical six-phase induction machine (right).

while the torque equation takes the form

$$T_{\mathrm{e}} = PL_{\mathrm{m}}[i_{d\mathrm{r}}i_q^{\mathrm{INV}} - i_q^{\mathrm{INV}}i_{q\mathrm{r}}] \tag{14}$$

Model (12)–(14) in the stationary reference frame shows once more that the rotor of the six-phase machine is coupled only with inverter *d*–*q* currents. Consequently, inverter *d*–*q* currents govern the torque and air-gap flux production of the six-phase machine. Since the *d*–*q* stator and rotor equations, as well as the torque expression, are identical to those of a three-phase machine, the same vector control schemes can be used. However, the additional degrees of freedom that exist in a symmetrical six-phase machine (*x*–*y* components and 0− component in the case of a single star point) make any attempt to control only two stator current components (*d*–*q* in the rotating reference frame or α–β in the stationary reference frame) inappropriate (unless a suitable SVM technique is devised), as already discussed in the previous sub-section. As a consequence, it is necessary to control at least four current components (if there are two isolated stator winding star points) or five current components (when there is a single isolated star point). Control of the required number of currents can be most easily accomplished by utilising current control in the stationary reference frame, in conjunction with phase inverter currents, as discussed next.

4. Control of the six-phase induction motor

As the model (12)–(14) indicates, the symmetrical six-phase induction machine can be controlled using rotor flux oriented control principles. Indirect (feed-forward) rotor flux oriented control is considered and current control in the stationary reference frame is assumed, exercised upon the inverter phase currents. The vector controller in Fig. 1 is of the same structure as for a three-phase machine and is illustrated in Fig. 2. Individual phase current references of the machine are given with ($k = \sqrt{2/6}$):

$$\begin{aligned}
i_{\mathrm{A}}^* &= i_{\mathrm{as}}^* = k[i_{ds}^* \cos\phi_{\mathrm{r}} - i_{qs}^* \sin\phi_{\mathrm{r}}] \\
i_{\mathrm{B}}^* &= i_{\mathrm{bs}}^* = k[i_{ds}^* \cos(\phi_{\mathrm{r}} - \alpha) - i_{qs}^* \sin(\phi_{\mathrm{r}} - \alpha)] \\
&- \\
i_{\mathrm{F}}^* &= i_{\mathrm{fs}}^* = k[i_{ds}^* \cos(\phi_{\mathrm{r}} - 5\alpha) - i_{qs}^* \sin(\phi_{\mathrm{r}} - 5\alpha)]
\end{aligned} \tag{15}$$

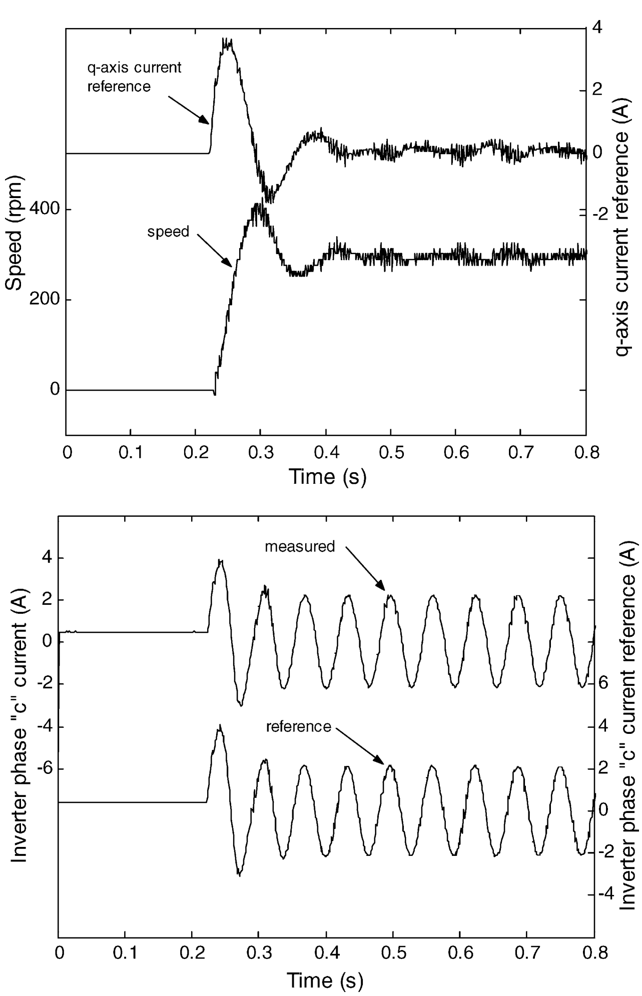

Fig. 4. Drive response for acceleration transient, 0–300 rpm.

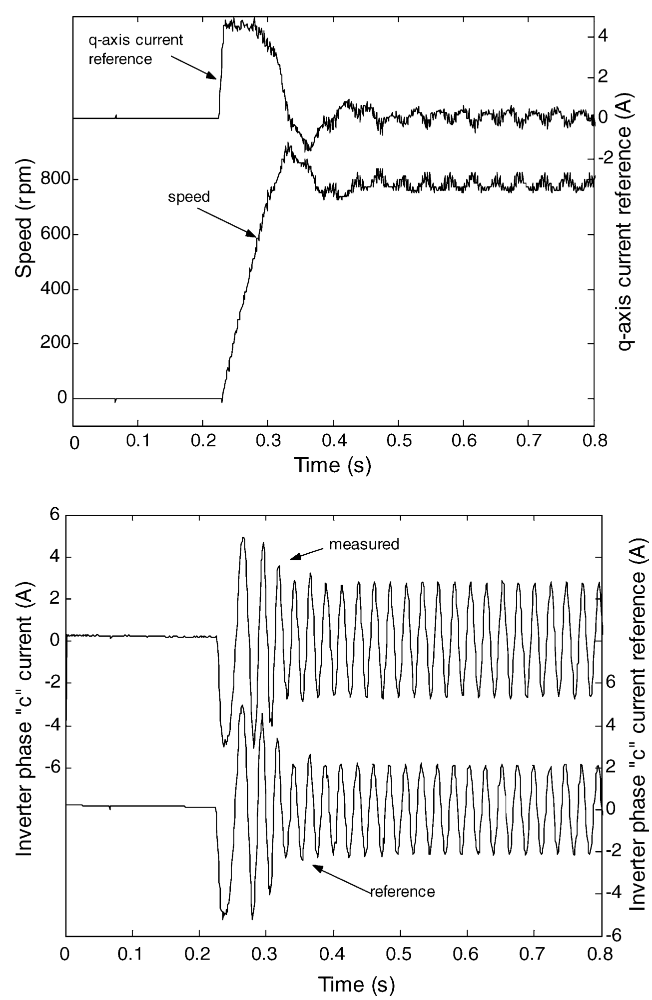

Fig. 5. Drive response for acceleration transient, 0–800 rpm.

It is important to note that the co-ordinate transformation of (15) *automatically* sets reference values for stator current components for x–y and 0+ to 0− circuits to zero. Hence, provided that the current control is sufficiently good, neither harmonics of the order $6n \pm 1$ ($n = 1, 3, 5, \ldots$) nor harmonics of the order $3n$ will be generated by the inverter, since inverter phase current references (15) are in any steady state pure sinusoidal functions. The same current control principle is directly applicable to an asymmetrical six-phase machine.

5. Experimental test bench

The experimental set-up, illustrated in Fig. 3, utilises two three-phase industrial-grade inverters. The inverters are paralleled to the same dc link. The inverters are rated at 14/42 A/A (continuous rms/peak). Each of them is equipped with a Texas Instruments' TMS320F240 DSP. The first three-phase inverter supplies phases A, C and E, while the second inverter supplies phases B, D and F. All six currents are measured using LEM sensors. Current control rate and inverter switching frequency are 10 kHz. PWM ripple is filtered out in the DSPs using FIR filters, which average 2^n equidistant samples taken during one switching period. Current signal, which is now PWM-ripple-free, is further used as the input of the current controllers. The inverter DSPs perform closed loop phase current control in the stationary reference frame, using digital form of ramp-comparison PWM with PI controllers in the most basic form [21]. Hence, the problem of deviation of the actual motor phase current with respect to its reference will be experienced at higher operating frequencies [21]. This could be removed by employing improved current regulators [22]; however, such a modification of the current controllers is beyond the scope of this paper.

The inverter current references are passed to the DSPs from a PC, through a dedicated interface card. The control code is written in C. It performs closed loop speed control and indirect rotor flux oriented control according to Fig. 2. Phase current references are calculated using (15).

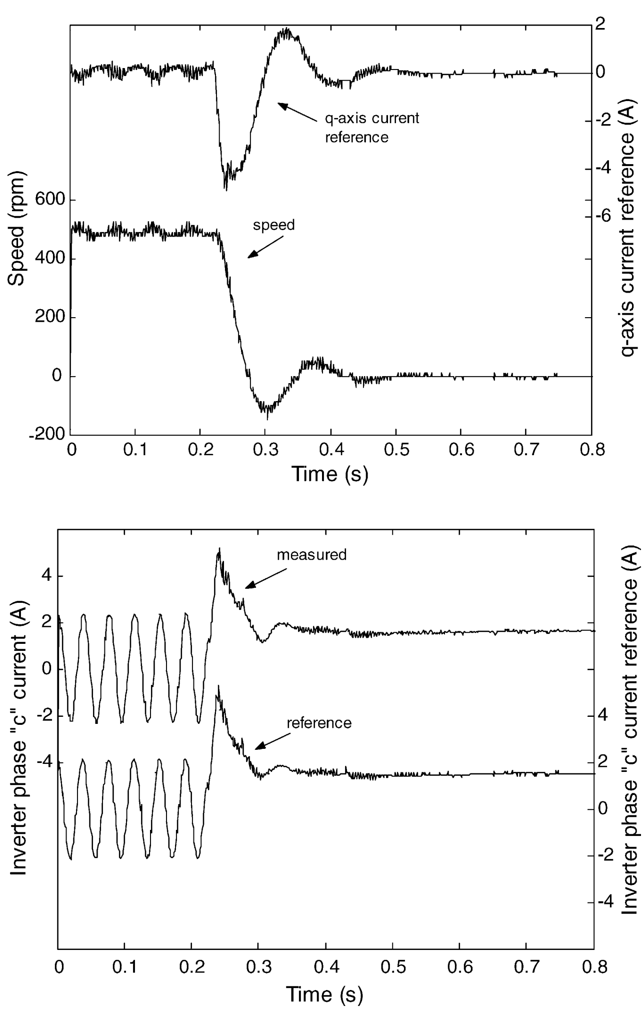

Fig. 6. Drive behaviour during deceleration from 500 down to 0 rpm.

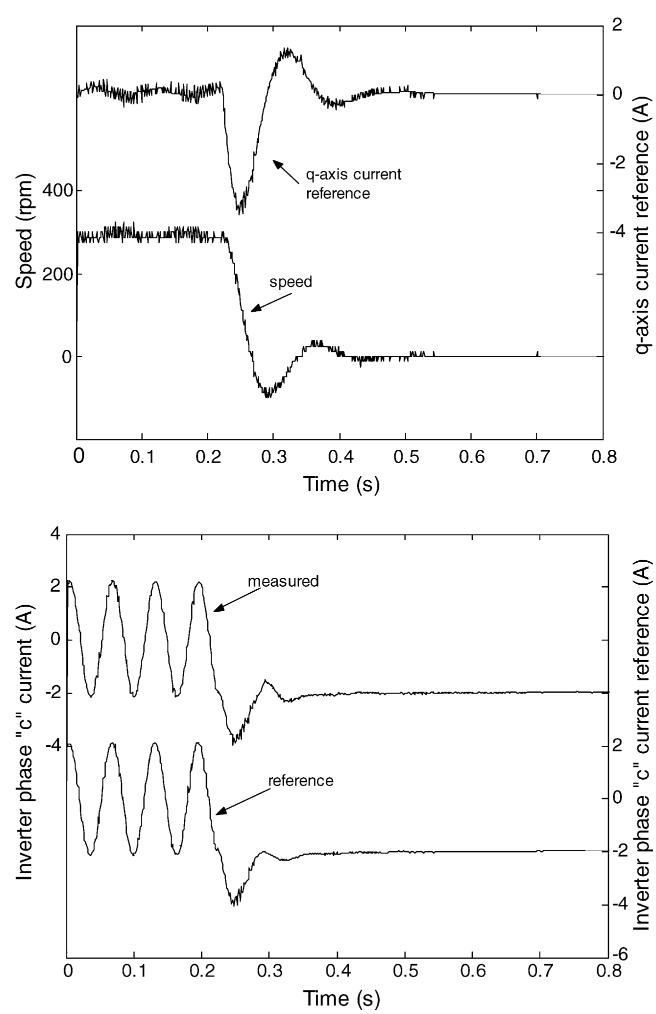

Fig. 7. Drive behaviour during deceleration from 300 down to 0 rpm.

The symmetrical six-phase induction machine is obtained by rewinding the stator of a three-phase machine and is 50 Hz, six-pole. Rated phase-to-neutral voltage is 110 V and other relevant ratings are 1.1 kW, 2.7 A, 900 rpm. Details of the stator winding are provided in Appendix A. Position is measured with a resolver and control operates in speed-sensored mode.

A series of experimental tests are performed in order to examine the dynamics of the drive and current control properties. Constant flux operation in the base speed region, with constant stator d-axis current reference of 1.5 A (rms), is examined. This value is 14% lower than the rated magnetizing current (1.75 A), since an attempt was made to avoid operation of the machine in the saturated region of the magnetizing curve (this is a potential source of detuned operation, which can impact on both dynamics and steady state operation, since it affects the value of the rotor time constant). The required value of the rotor time constant (i.e., slip gain) was established through on-line testing, using the principle that the correct slip gain provides practically linear speed response to a step speed command change. Stator q-axis current reference limit is set to 3.5 A (rms). This corresponds to the maximum dynamic torque of just below 1.5 times the rated motor torque. Special attention is paid to the actual current waveform, since the reference currents are pure sine waves in any steady state. The results are reported in the following section.

6. Experimental results

The results of the experimental study are illustrated for all transients by displaying the speed response, stator q-axis current reference (peak value), and actual and reference current for one inverter (stator) phase. A step speed reference change is initiated in all cases. The machine is coupled to a dc machine, thus providing an increased inertia. It operates under no-load conditions except for loading and unloading tests.

Acceleration transients, starting from standstill, are shown in Figs. 4 and 5. The speed reference setting is 300 and 800 rpm, respectively. Typical behaviour of a vector

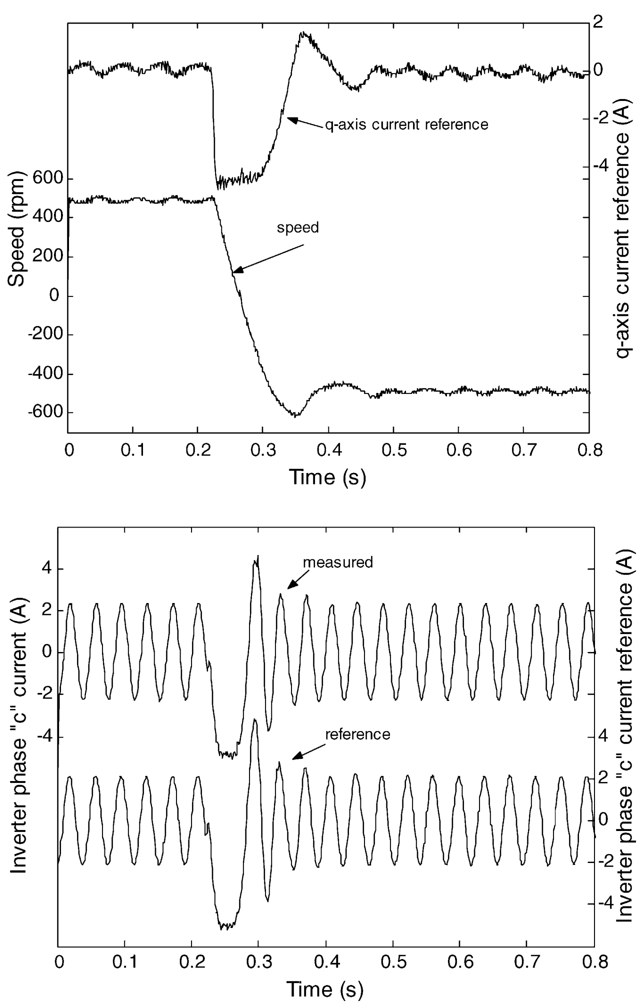

Fig. 8. Speed reversal from 500 to −500 rpm.

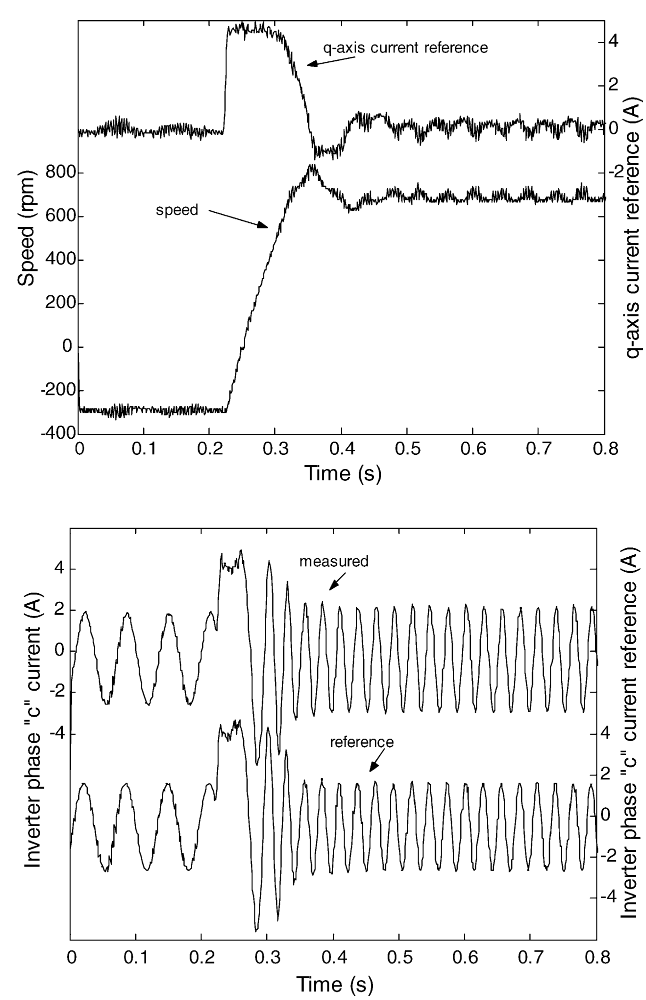

Fig. 9. Speed reversal from −300 to 700 rpm.

controlled induction machine is observed, with rapid stator q-axis current reference build-up corresponding to almost instantaneous torque build-up. Speed response is therefore the fastest possible for the given current limit. Stator phase current reference and the actual current are in excellent agreement and closely correspond one to the other for final steady state at 300 rpm, while at 800 rpm there is some discrepancy which is in agreement with findings of [21].

The second test is a deceleration transient, illustrated in Figs. 6 and 7. The machine is decelerated from 500 rpm and 300 rpm, respectively, down to zero speed. The same quality of performance as for the acceleration transient is obtained.

The next two sets of results illustrate reversing transients. Transition from 500 to −500 rpm is shown in Fig. 8, while Fig. 9 illustrates speed reversal from −300 to 700 rpm. Prolonged operation in the stator current q-axis current limit results in both cases, leading to rapid change of the direction of rotation.

Measured phase current and reference phase current are in excellent agreement in Fig. 8, while in Fig. 9 some amplitude related discrepancy can be again observed at 700 rpm, this being a consequence of the applied simplest method of digital ramp comparison control [21]. However, what is very important to note is that actual current in all steady states at non-zero frequency in Figs. 4–9 contains essentially only the fundamental harmonic. Low order harmonics practically do not appear in the actual current and this confirms that the problems caused by low order harmonics of the order $6n \pm 1$ ($n = 1, 3, 5, \ldots$), reported in [15–17], can be successfully eliminated by the current control method applied here. Hence, harmonic elimination filters of the type proposed in [23] or dedicated inverter PWM methods, such are those of [14,17], are not required.

To further corroborate this statement, some additional steady state current measurements are conducted using Tektronix current probe A6302 (with AM 503A current amplifier) and HP digital spectrum analyser HP 35665A. The machine runs still under no-load conditions and the stator d-axis current reference setting is still 1.5 A rms. Time domain current waveforms and associated low frequency

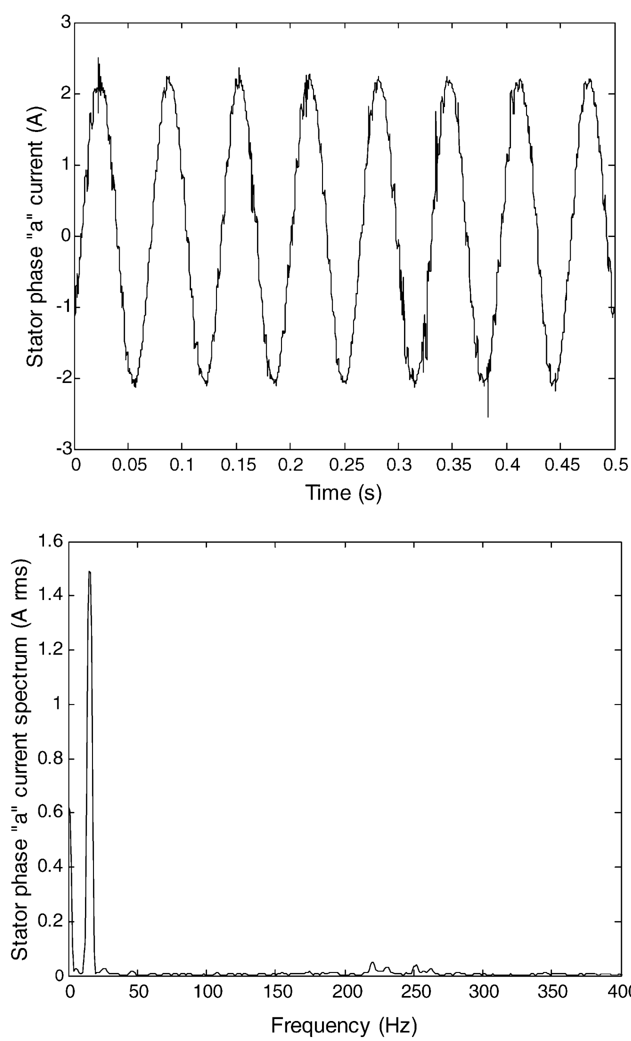

Fig. 10. Steady state phase current and its spectrum at 300 rpm (15 Hz).

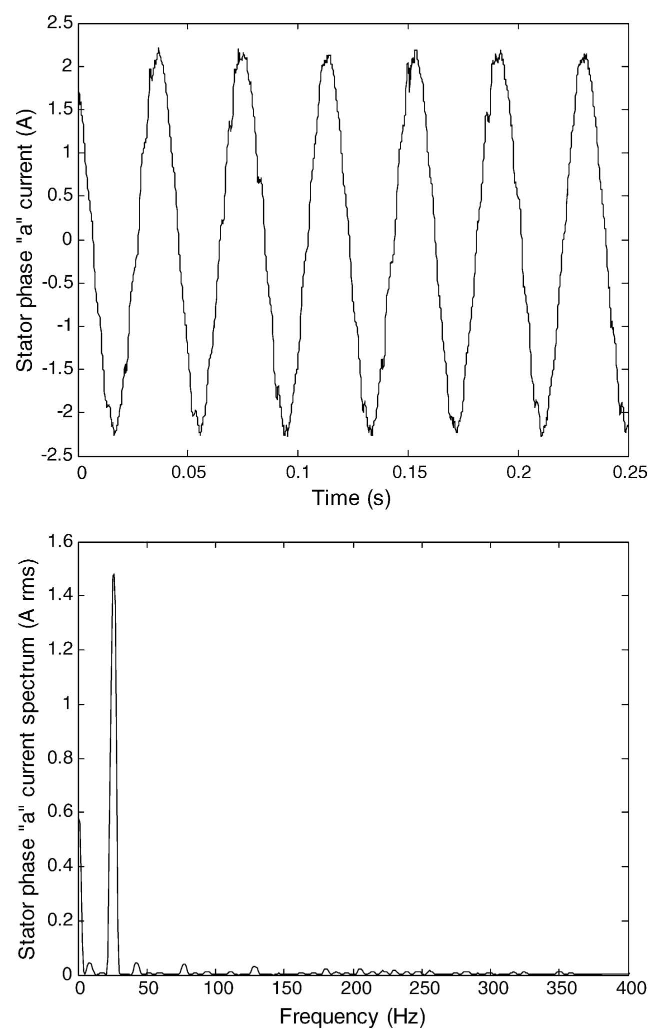

Fig. 11. Steady state phase current and its spectrum at 500 rpm (25 Hz).

parts of the spectra are displayed in Figs. 10–12 for operation at 15, 25 and 40 Hz, respectively. As can be seen from Figs. 10 and 11, low-order current harmonics are practically non-existent at low to medium operating frequencies, confirming the ability of the adopted current control scheme to eliminate unwanted *x*–*y* and zero sequence harmonics. At higher frequencies one can observe appearance of some lower order harmonics (Fig. 12). These are, however, of negligibly small amplitudes. It should be noted that the fundamental current component at 15 and 25 Hz closely corresponds to the stator *d*-axis current reference of 1.5 A rms, while at 40 Hz it is slightly higher due to the more significant no-load losses (*q*-axis current) and due to the ramp-comparison current control.

Finally, the last two experiments, illustrated in Figs. 13 and 14, show the drive behaviour during step loading and step unloading, respectively. Fig. 13 applies to operation at 300 rpm, while step unloading in Fig. 14 takes place at 600 rpm. It can be seen from these two figures that the drive disturbance rejection capability is excellent and commensurate with expected performance of a vector-controlled drive.

Presented experimental results indicate existence of a certain ripple in the stator *q*-axis current, in addition to the measurement noise, observable at medium and higher speeds of rotation. The frequency of this stator *q*-axis current (torque) ripple is estimated from the presented experimental results under no-load conditions (Figs. 5, 6 and 8) as 2/3 of the fundamental operating frequency. Closer inspection of the current spectra at higher operating frequencies (Figs. 11 and 12) reveals the existence of sub-harmonics at frequencies of 1/3 and 5/3 of the fundamental. Since these two sub-harmonics cause fields that rotate in opposite directions, both lead to the torque ripple at 2/3 of the fundamental frequency. The appearance of these unwanted sub-harmonics is not related to any deficiencies in the current control. The source of sub-harmonics is believed to be rotor eccentricity, which can be avoided by a better design and assembly of the machine. This issue is currently under scrutiny and is beyond the scope of this paper.

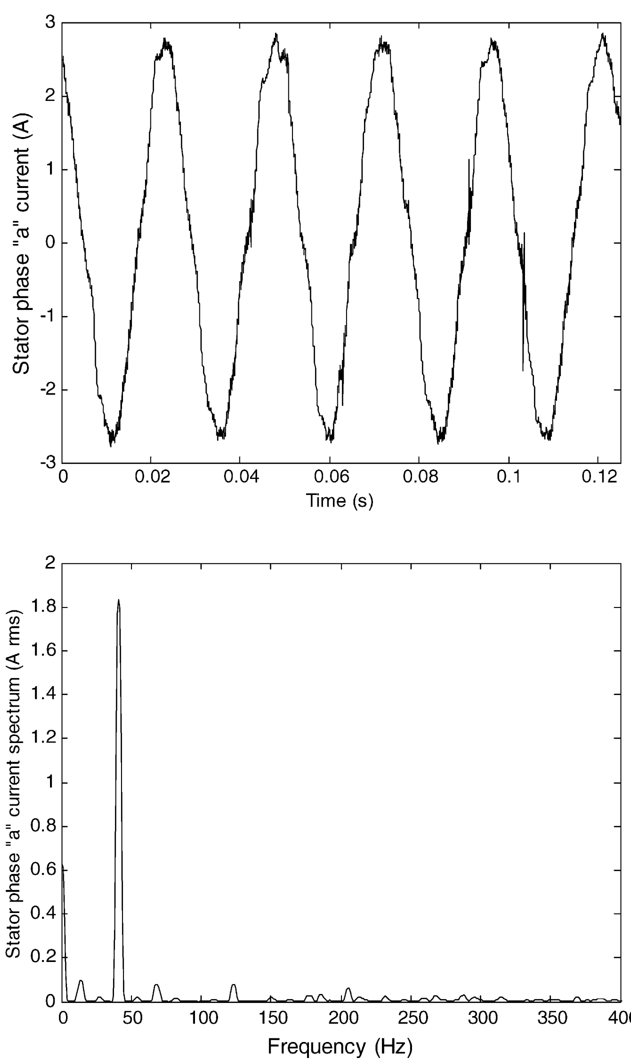

Fig. 12. Steady state phase current and its spectrum at 800 rpm (40 Hz).

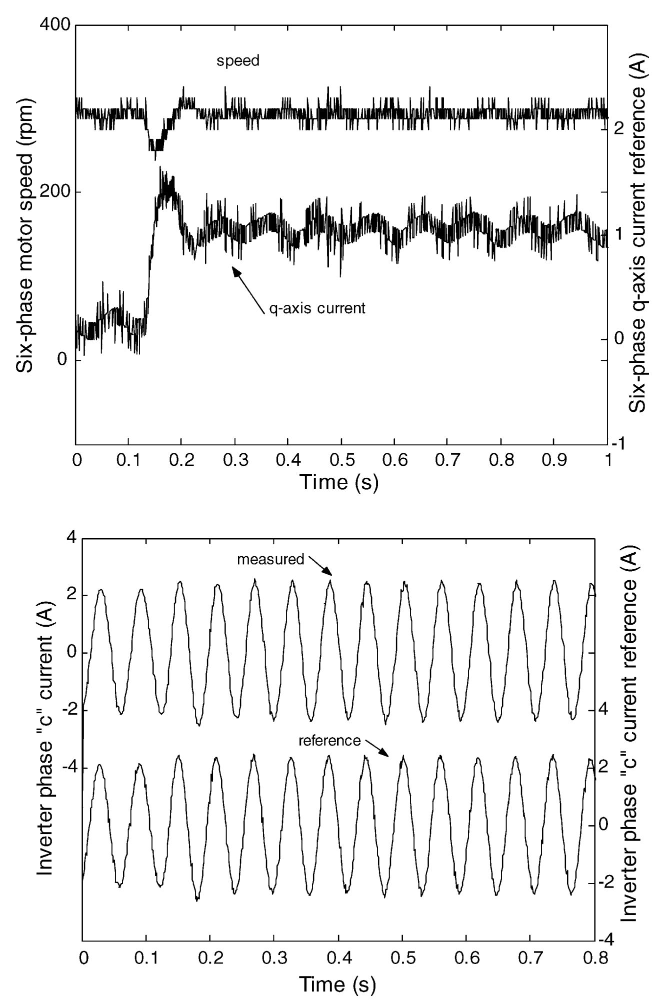

Fig. 13. Drive response during step loading at 300 rpm.

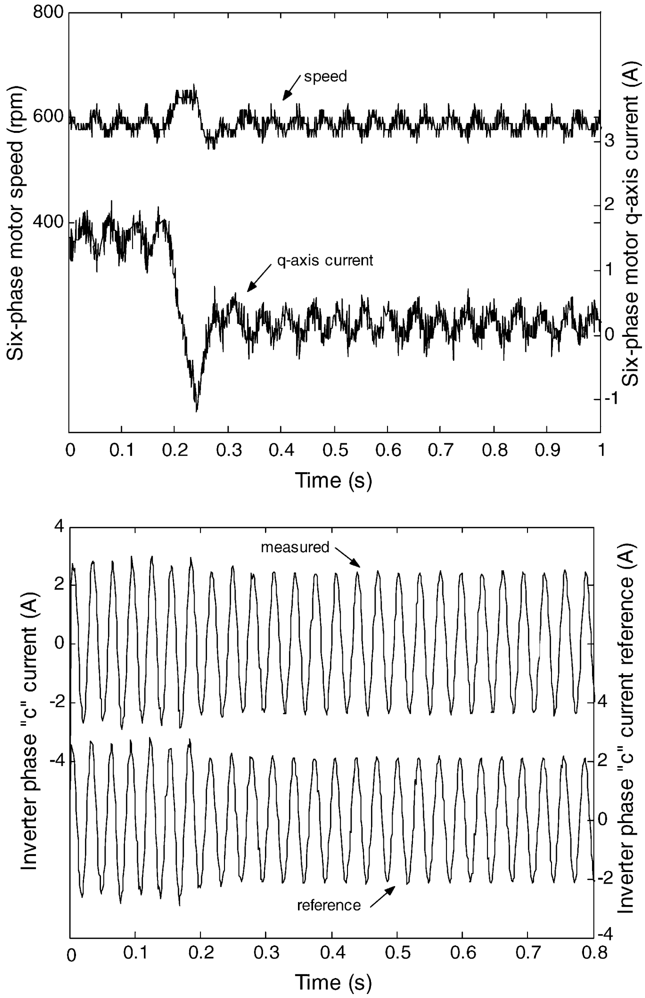

Fig. 14. Drive response during step unloading at 600 rpm.

7. Conclusion

The paper discusses indirect vector control of a symmetrical six-phase induction machine with a single isolated neutral point. A model of the machine is at first derived, on the basis of which it is concluded that: (i) an indirect vector control algorithm can be applied to achieve decoupled rotor flux and torque control in the same manner as it is done for a three-phase machine and (ii) it is not sufficient to control only two stator components in either rotating (d–q components) or stationary (α–β components) reference frame, unless the PWM scheme automatically provides zero voltage harmonics in x–y and zero-sequence sub-spaces. Problems with high values of stator current's low-order harmonics, reported in a number of surveyed references in conjunction with asymmetrical six-phase machines, were due to the inadequate inverter control.

It is reasoned that the unwanted harmonics, which can flow in x–y and 0+ to 0− circuits, can be most easily suppressed by implementing current control exercised upon phase currents. If the star points of the two three-phase windings are left isolated, four current controllers are sufficient. These conclusions are applicable to both asymmetrical and symmetrical six-phase machines and, indeed, in general to all machines with five phases or more, where the required number of current controllers will increase as the number of phases increases. The approach based on direct phase current control is therefore adopted for practical realisation.

The developed algorithm is further implemented in an experimental test bench and is verified by performing a number of tests. These include acceleration, deceleration, reversing and step loading/unloading transients. Excellent dynamics, commensurate with vector control algorithm, are demonstrated. It is also shown, by means of spectrum analysis, that application of the current control in conjunction with motor phase currents greatly alleviates the problem of low-order stator harmonic current flow in x–y and 0+ to 0− circuits.

Acknowledgement

The authors gratefully acknowledge financial support provided for the work on this project by the EPSRC, under the standard research Grant number GR/R64452/01 and by Semikron Ltd.

Appendix A. Six-phase machine stator winding details

Stator and rotor of the six-phase machine have 36 and 44 slots, respectively, and the machine is six-pole. Stator winding is of double-layer lap type. It is designed with a short pitch of 5/6. The wiring diagram, for the two phases in space opposition (B and E) is, in terms of slot numbers, as follows:

B1 to 27-32-28-33 to 15-20-16-21 to 3-8-4-9 to B2
E1 to 9-14-10-15 to 21-26-22-27 to 33-2-34-3 to E2

Here B1 and E1 are phase inputs and B2 and E2 are phase outputs. In each of the three-phase groups of a phase the conductors are in the upper layer in the first and the third slot and in the bottom layer in the second and the fourth slot. The winding function of phase B over one pole pair is illustrated in Fig. A.1. As is obvious from Fig. A.1, the winding function is asymmetrical, so that spatial distribution of the magneto-motive force contains even harmonics (but the lowest odd harmonics, the fifth and the seventh, are significantly attenuated by the selected short pitch of 5/6; had the pitch been selected as full, winding function would have been symmetrical, without even harmonics, but the low order odd harmonics would have been of significant values).

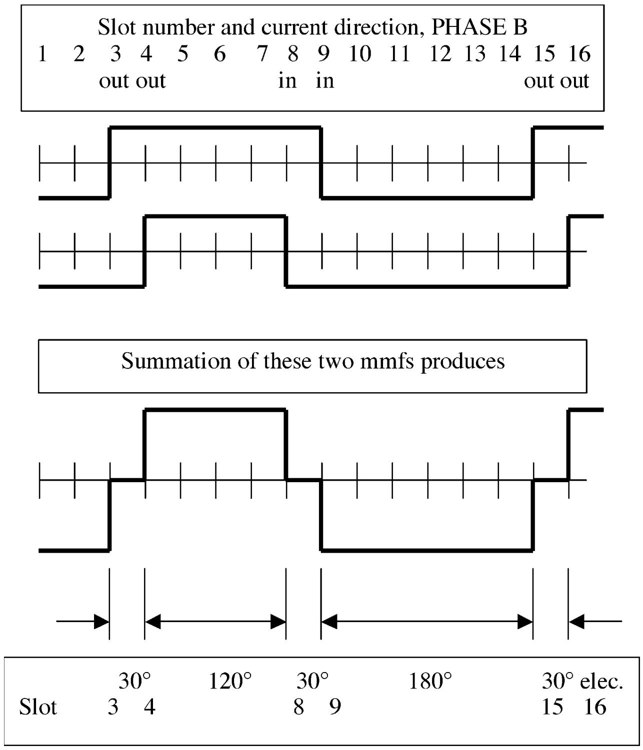

Fig. A.1. Winding function of phase B.

References

[1] E.E. Ward, H. Härer, Preliminary investigation of an invertor-fed 5-phase induction motor, Proc. IEE 116 (6) (1969) 980–984.

[2] M.A. Abbas, R. Christen, T.M. Jahns, Six-phase voltage source inverter driven induction motor, IEEE Trans. Ind. Appl. IA-20 (5) (1984) 1251–1259.

[3] K. Gopakumar, S. Sathiakumar, S.K. Biswas, J. Vithayathil, Modified current source inverter fed induction motor drive with reduced torque pulsations, IEE Proc. 131 (4) (1984) 159–164, Pt. B.

[4] S. Mantero, E. De Paola, G. Marina, An optimised control strategy for double star motors configuration in redundancy operation mode, in: Proceedings of European Power Electronics and Applications Conference EPE, Lausanne, Switzerland, CD-ROM Paper No. 013, 1999.

[5] M. Steiner, R. Deplazes, H. Stemmler, A new transformerless topology for ac-fed traction vehicles using multi-star induction motors, EPE J. 10 (3–4) (2000) 45–53.

[6] T.M. Jahns, Improved reliability in solid-state ac drives by means of multiple independent phase-drive units, IEEE Trans. Ind. Appl. IA–16 (3) (1980) 321–331.

[7] J.R. Fu, T.A. Lipo, Disturbance-free operation of a multiphase current-regulated motor drive with an opened phase, IEEE Trans. Ind. Appl. 30 (5) (1994) 1267–1274.

[8] S. Green, D.J. Atkinson, A.G. Jack, B.C. Mecrow, A. King, Sensorless operation of a fault tolerant PM drive, IEE Proc. Electr. Power Appl. 150 (2) (2003) 117–125.

[9] D. Hadiouche, H. Razik, A. Rezzoug, On the modelling and design of dual-stator windings to minimize circulating harmonic currents for VSI fed ac machines, IEEE Trans. Ind. Appl. 40 (2) (2004) 506–515.

[10] R. Bojoi, M. Lazzari, F. Profumo, A. Tenconi, Digital field-oriented control for dual three-phase induction motor drives, IEEE Trans. Ind. Appl. 39 (3) (2003) 752–760.

[11] B. Stumberger, G. Stumberger, A. Hamler, M. Trlep, M. Jesenik, V. Gorican, Increasing the output power capability in a six-phase flux-weakened permanent magnet synchronous motor with a third harmonic current injection, IEEE Trans. Magnetics 39 (5) (2003) 3343–3345.

[12] R.O.C. Lyra, T.A. Lipo, Torque density improvement in a six-phase induction motor with third harmonic current injection, IEEE Trans. Ind. Appl. 38 (5) (2002) 1351–1360.

[13] R. Bojoi, F. Farina, A. Tenconi, F. Profumo, E. Levi, Stationary frame digital current regulation for dual-three phase induction motor drives, in: Proceedings of IEEE Power Electronics Specialists Conference PESC, Aachen, Germany, 2004, pp. 2121–2127.

[14] Y. Zhao, T.A. Lipo, Space vector PWM control of dual three-phase induction machine using space vector decomposition, IEEE Trans. Ind. Appl. 31 (5) (1995) 1100–1109.

[15] K. Gopakumar, V.T. Ranganathan, S.R. Bhat, Split-phase induction motor operation from PWM voltage source inverter, IEEE Trans. Ind. Appl. 29 (5) (1993) 927–933.

[16] K. Gopakumar, V.T. Ranganathan, S.R. Bhat, Vector control of induction motor with split-phase windings, EPE J. 7 (1–2) (1997) 61–66.

[17] K.K. Mohapatra, K. Gopakumar, V.T. Somasekhar, L. Umanand, A harmonic elimination scheme for an open-end winding induction motor drive, IEEE Trans. Ind. Electron. 50 (4) (2003) 1187–1198.

[18] R.H. Nelson, P.C. Krause, Induction machine analysis for arbitrary displacement between multiple winding sets, IEEE Trans. Power Apparatus Syst. PAS-93 (1974) 841–848.

[19] E.A. Klingshirn, High phase order induction motors. Part I. Description and theoretical considerations, IEEE Trans. Power Apparatus Syst. PAS-102 (1) (1983) 47–53.

[20] R. Bojoi, A. Tenconi, F. Profumo, Digital synchronous frame current regulation for dual-three phase induction motor drive, in: Proceedings of IEEE Power Electronics Specialists Conference PESC, Acapulco, Mexico, 2003, pp. 1475–1480.

[21] D.M. Brod, D.W. Novotny, Current control of VS-PWM inverters, IEEE Trans. Ind. Appl. 21 (4) (1985) 562–570.

[22] T.M. Rowan, R.J. Kerkman, A new synchronous current regulator and an analysis of current-regulated PWM inverters, IEEE Trans. Ind. Appl. IA-22 (4) (1986) 678–690.

[23] E.A. Klingshirn, Harmonic filters for six-phase and other multi phase motors on voltage source inverter, IEEE Trans. Ind. Appl. IA-21 (4) (1985) 588–593.